Characterization and Potential Industrial Applications of Kaolinite from Argungu, Kebbi State, Nigeria

John Augustine Lawal[1], Omolola Titilayo Odeyemi[2], Temitope Emmanuel Anaun[1], Folashade Habibat Omotehinwa[1]

[1]Department of Industrial Chemistry, Achievers University, Idesen-Ute Road, Owo, P.M.B. 1030 Owo, Ondo State, Nigeria

[2]Department of Science Laboratory Technology, Kwara State Polytechnic, Ilorin, Kwara State, Nigeria

Corresponding author: lawal.ja@achievers.edu.ng (Tel: +2348030681269)

ABSTRACT: The characteristics of clay from Argungu deposit, Kebbi State, Nigeria was investigated to determine its potential industrial applications. The analysis of the purified 63 µm fraction of the clay was carried out using X-ray Diffraction (XRD), Fourier Transform Infrared Spectroscopy (FTIR), Scanning Electron Microscopy/Electron Dispersive X-Ray Spectroscopy (SEM/EDS) and Thermogravimetry/Differential Scanning Calorimetry (TGA/DSC) techniques. The XRD patterns and infrared absorption bands results confirmed kaolinite as only clay mineral present in the purified sample. The isotherm parameters classified the kaolinite structure as mesoporous, type IV and hysteresis pattern of type H3. The clay orientation exhibit non-uniform size aggregate layers of particle. The mineralogical and elemental composition, morphology, thermal stability, alumina and silica content, low or absence of toxic ions are characteristics that offer the clay as a vital raw material for wide range of industrial applications.

Keywords: Clay, characterization, industrial application, kaolinite, mineralogical composition.

1. INTRODUCTION

Kaolin is a white, soft and plastic hydrated aluminum silicate clay mineral with the ideal formula of $Al_2Si_2O_5(OH)_4$. The kaolin group including kaolinite, dickite, nacrite and halloysite are formed by the decomposition of orthoclase feldspar. Kaolinite is the most common member of the group with dominant type 1:1 phyllosilicate of two fundamental crystal sheet as tetrahedral or silica and octahedral or alumina sheet. In a unit structure, one octahedral sheet is linked with the apical oxygen ion of the tetrahedral [l]. In Nigeria, an estimated three billion metric tonnes of kaolin is found in deposits across the regions of the country [2].

The multiplicity of industrial application of kaolin clay is basically due to its favourable physical and chemical properties. It a potential raw material in paper, ceramic, petroleum, catalyst, adsorbent, plastic, paint, ink, and pharmaceutical while new application are still been discovered. Kaolin clay have satisfactorily served the demand for filler, paper and ceramic industries [3], adsorption of heavy metal [4-6] and catalysts [7].

In this study, the characterization of the clay was carried out to determine the mineralogical and elemental composition, morphology, thermal stability and to predict the possible industrial applications based on its fundamental properties.

2. EXPERIMENTAL

2.1 Clay Sampling and Purification

Sampling: The clay sample was obtained from a deposit at Arugungu, Kebbi State; an extension of Sokoto sedimentary basin, Nigeria (12.7495^o N and 4.5367 ^{o} E). The sample was obtained by taking properly mixed representative samples using the cone and quartering techniques.

Purification of Clay Sample: The obtained sample was pulverized, suspended in deionized water for 12 hours and the particles disaggregated using agitator probe. The clay particles in the slurry was

sieved through 63µm sieve to remove sand particles and other impurities. The clay particles in the filtrate was sedimented by centrifugation for 30 minutes at the rate of 3500 revolution per minute and dried in an oven at 105 ^{0}C for 1 hour.

2.2 Characterization Methods

Characterization of the purified clay sample was carried out using analytical standard procedures. The determination of the qualitative and quantitative mineralogical phase composition of the sample was carried out with an X-Ray Diffractometer (BRUKER, AXS D8 Advance) using copper Kα radiation (λ Kα_1 = 1.5406Å) at measurement time of 0.5 sec/step in the interval (2 theta range) of 5 – 80^o. The Infrared spectrum of the clay from Bruker Tensor 27 Platinum ATR-FTIR, operated in the infrared region of 400 to 4000 cm^{-1}. The morphology of the clay sample was imaged using TESCAN VEGA TS 5136LM Scanning Electron Microscope (SEM) interphase with Electron Dispersive X-ray Spectrometer (EDS) to determine its elemental composition. The clay particle surface area, pore-volume and pore sizes were determined using Micrometrics Type Tristar II 3020 Surface Area Analyzer. Perkin-Elmer TGA 7 Thermal Gravimetric/Differential Scanning Calorimetry Analyzer (TGA/DSC) was used to determine the mass and phase changes as a function of temperature.

3. RESULTS AND DISCUSSION

3.1 XRD Characterization

The diffraction patterns for the faces of the Argungu clay particles showed basal peaks of 001, 002, 003 and 004 at 2θ values of 12.5, 19.8, 37.8 and 51^0 respectively. The prism peaks for the edges of the clay particles were 020, 110, 130 and 202 at their relative 2θ values of 19.8, 20, 35, and 38.5^0 respectively (Fig 1). These reflection peaks for the interlayer spacing confirms kaolinite as the only clay mineral present in the 63 µm fraction of Argungu clay. Similar basal and prism diffraction peaks for kaolinite have been reported in literature [8, 9].

3.2 FTIR Analysis

The result of the FTIR spectrum of the clay is presented in Fig 2. The infrared absorptions were characterized by two strong bands at 3687.40 and 3619.93 cm^{-1} representing in-phase symmetric stretching vibration of surface hydroxyl groups and inner hydroxyl groups between the tetrahedral and octahedral sheet. These absorption bands, reaffirm Argungu clay as kaolinite. Strong infrared absorptions in the range of 1000 to 400cm^{-1} indicates; in-plane Si-O stretching assignment, deformation bands of inner-surface hydroxyl groups, Al-O bands and deformation bands of Al-O-Al and Si-O-Si (Table 1). Similar IR assignment for kaolinite have been reported in literature [10-12].

3.3 Surface Area and Adsorption-Desorption Isotherm

The surface area pore structure parameter results of the clay are presented in Fig 3 and 4. The surface area values obtained from single point, Brunauer-Emmett-Teller (BET) measurement, Langmuir and t-plot (statistical thickness of adsorbed multilayer on the pore surface area) were 21.36 m^2/g, 6.29 m^2/g, 65.20 m^2/g and 25.54 m^2/g respectively. Dubinin-Astakhov micro-pore surface area and average nanoparticle size were 34.08 m^2/g and 95.31 nm respectively. The determination of pore-size in the intermediate range was calculated using Barrett, Joyner and Halenda (BJH) method. The (BJH) adsorption and desorption surface area of pore obtained were 26.13 and 30.33 m^2/g with pore volume distribution values (pore diameter range from 1.7 to 300 nm) of 0.038 and 0.043 cm^3/g respectively. The BJH adsorption and desorption average pore width were 5.87 nm and 5.70 nm respectively. The adsorption-desorption isotherm plot (Fig 3), classified the pure clay as typical of mesoporous structure (type IV isotherm) based on IUPAC recommendation. The hysteresis pattern is of type H3; typical of agglomerates of plate-like clay particles [13, 14]. The t-plot (Fig 4), showed an initial linear region which extend only at short range and deviated upward at higher values of *t*. This indicate that the clay is mesoporous and is associated with capillary condensation [15, 16].

3.4 SEM-EDS Analysis

The SEM morphology of the clay as shown in Fig 5, revealed the structural orientation of Argungu clay predominantly exhibit aggregate layers of non-uniform size euhedral particles. Similar kaolin morphology have been reported in literature [17, 18]. The elemental composition of the clay obtained from the electron diffraction spectrum (Fig 6), showed the predominant elements as aluminum, silicon and oxygen with weight percentage of 19.06 %, 22.10 % and 71.06 % respectively. Other elements present in very low weight percentage composition are potassium (0.20 %), calcium (0.21 %), titanium (0.20 %) and iron (0.95 %) respectively.

3.5 TGA-DSC Thermogram

The TGA/DSC thermal curves of the clay measured from ambient to 600 ^{0}C at heat flow rate range of zero to 2.5 w/g is shown in Fig 7. The thermogram curves indicates an initial rapid loss in weight of 7.5 % at temperature of up to 125 ^{0}C due to loss adsorbed water molecules on the surface and interlayer lattice space of the clay. The second stage intensive weight loss of 8.75 % between 375 and 525 ^{0}C correspond to dehydroxylation of structural water in the octahedral layer. The DSC endothermic peak at 50 ^{0}C, confirms the structural adjustment that toke place due to dehydration of water held at the interlayer space of the lattice structure. Endothermic phase transition peak corresponding to dehydroxylation resulting to formation of meta-kaolinite crystals occurred at 475 ^{0}C. The temperature range at which the dehydration and dehydroxylation occurred is in reasonable agreement with literature [19, 20].

3.6 Potential Industrial Application

The characteristic features obtained from the characterization of Argungu kaolinite, showed the clay meets specification for wide range of industrial application. Its relatively large surface area, fine particle size, very low iron content and absence of toxic ions makes it useful for adsorption of

pollutants and potential raw material in paint, paper, cosmetics and as carriers for drug delivery system in pharmaceutical [21-24]. The high composition of silica and alumina content, low alkaline and iron content, low dehydroxylation temperature and very low titanium oxide compositions in the clay fit its application in synthesis of alumina and zeolite catalysts and production of ceramics [25, 26].

4. CONCLUSION

The results of the characterization of the purified Argungu clay shows the clay mineralogical composition is 100 % kaolinite. Favourable properties such as high alumina and silica content, very low iron and titanium content, unique softness, fine particle size and non-abrasiveness of Argungu kaolinite satisfy its multiplicity applications: as an adsorbent in wastewater treatment, synthesis of alumina and zeolite catalysts, extender pigment in paint, special filler in paper making, bio-ceramic and wall titles and cosmetics and pharmaceutical industries.

Table 1. Important Vibrational Band Assignment of the purified Argungu kaolinite

Wavenumber (cm^{-1})	Assignment
3687.40	Al-O-H stretching
3619.93	Al-OH (inter-octahedral)
1651.20	H-O-H
1114.26	Si-O-Si
1026.28	Si-O-H
1000.74	Si-O
909.81	Al-O-Al
749.28	Al-O
641.34	Si-O-Al
526.35	Si-O-Si
422.06	Si-O-Al

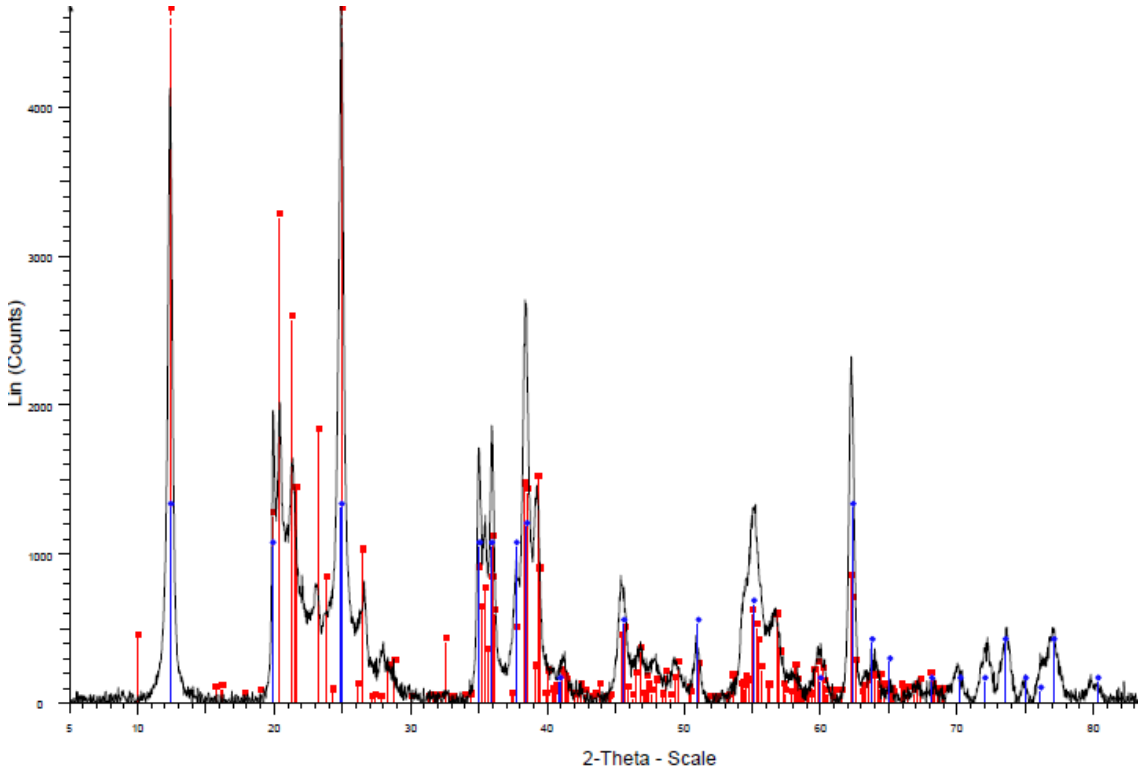

Figure 1: XRD pattern of the purified Argungu kaolinite

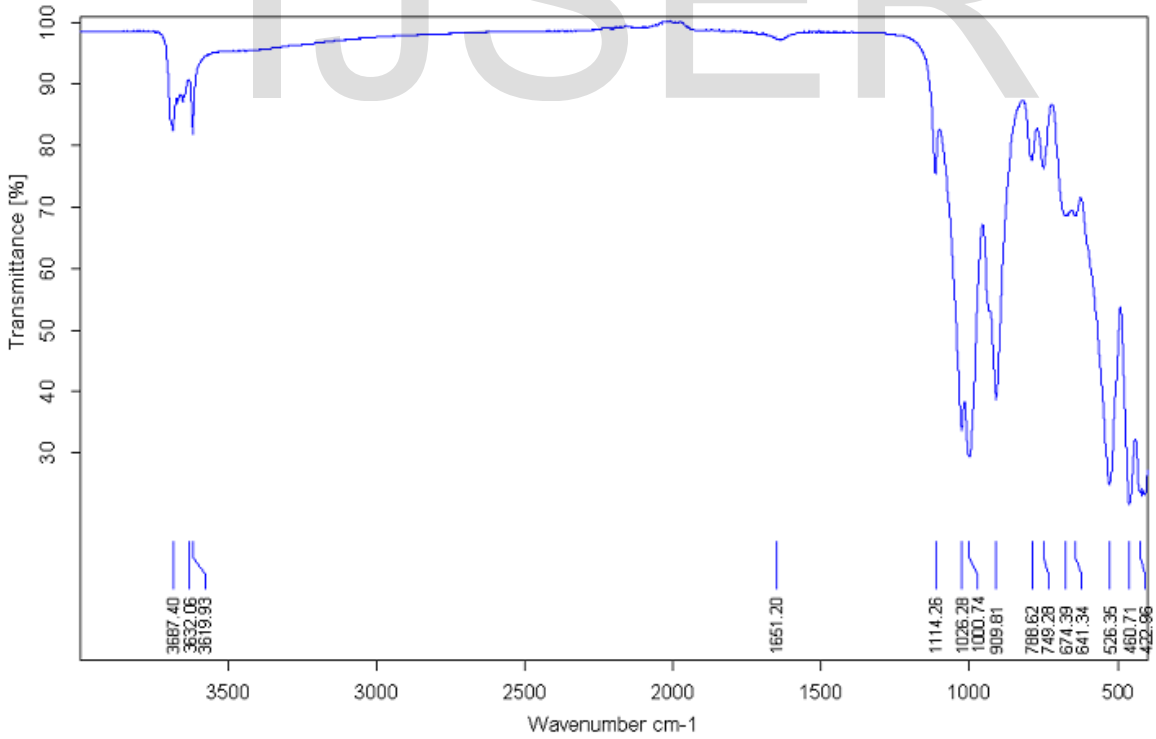

Figure 2: FTIR spectrum of the purified Argungu kaolinite

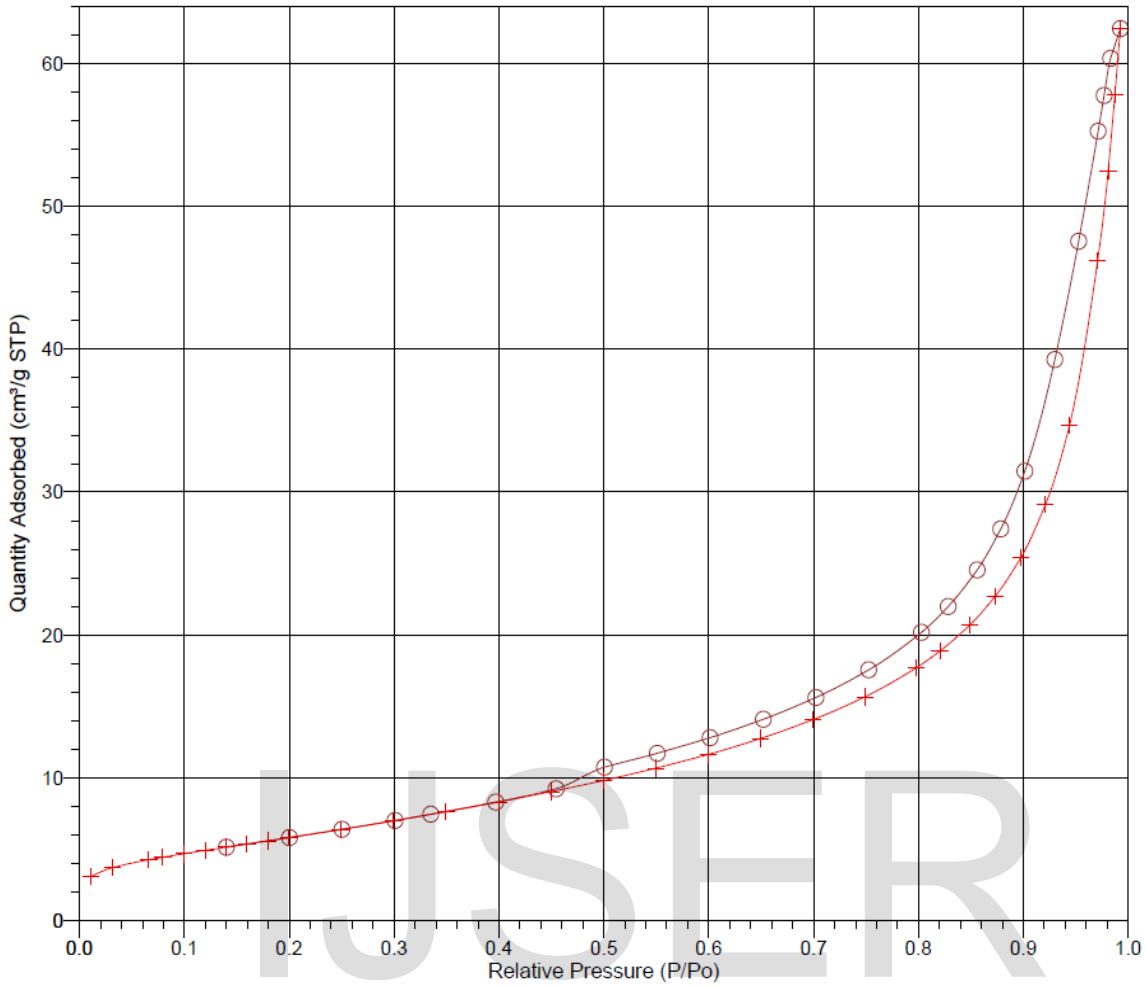

Figure 3: Nitrogen adsorption and desorption isotherm plot for the purified kaolinite

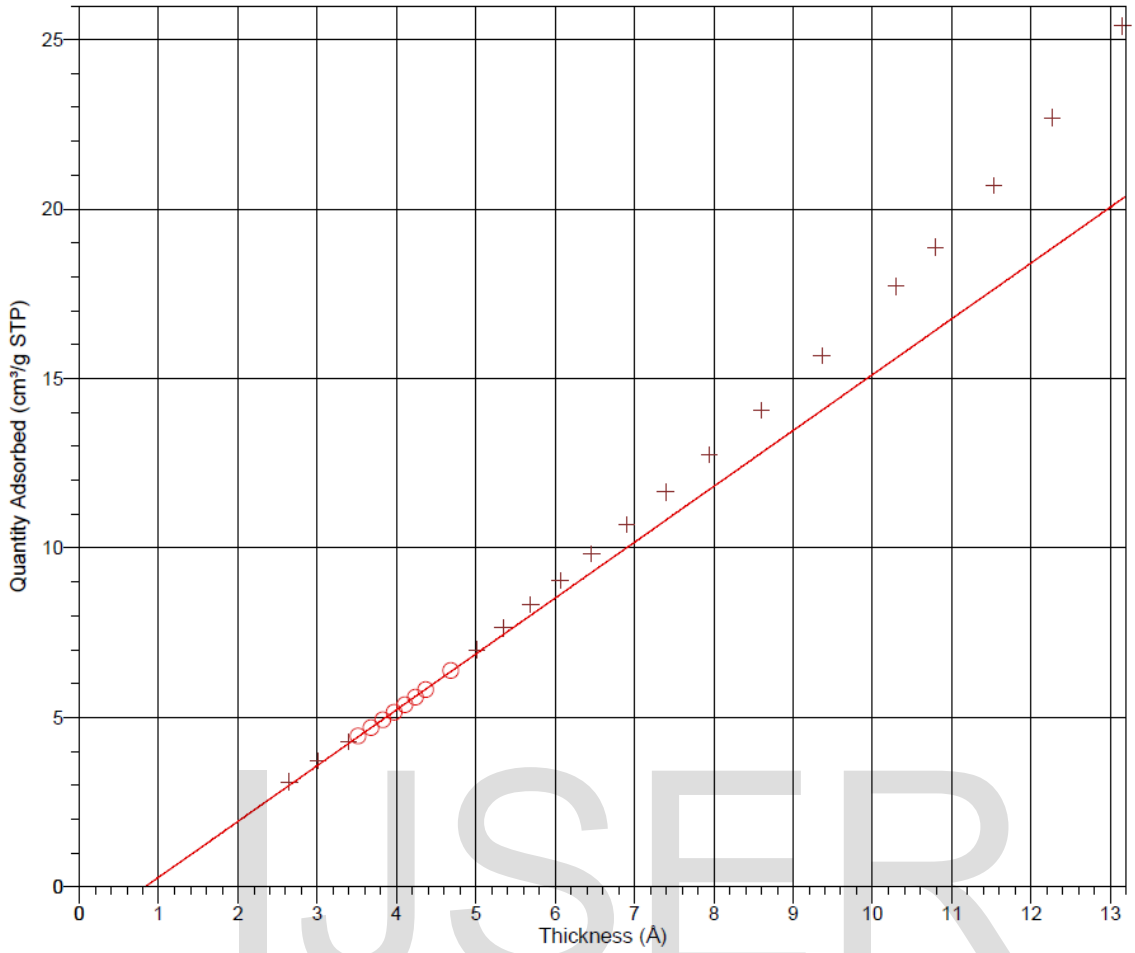

Figure 4: t-Plot for the purified Argungu kaolinite

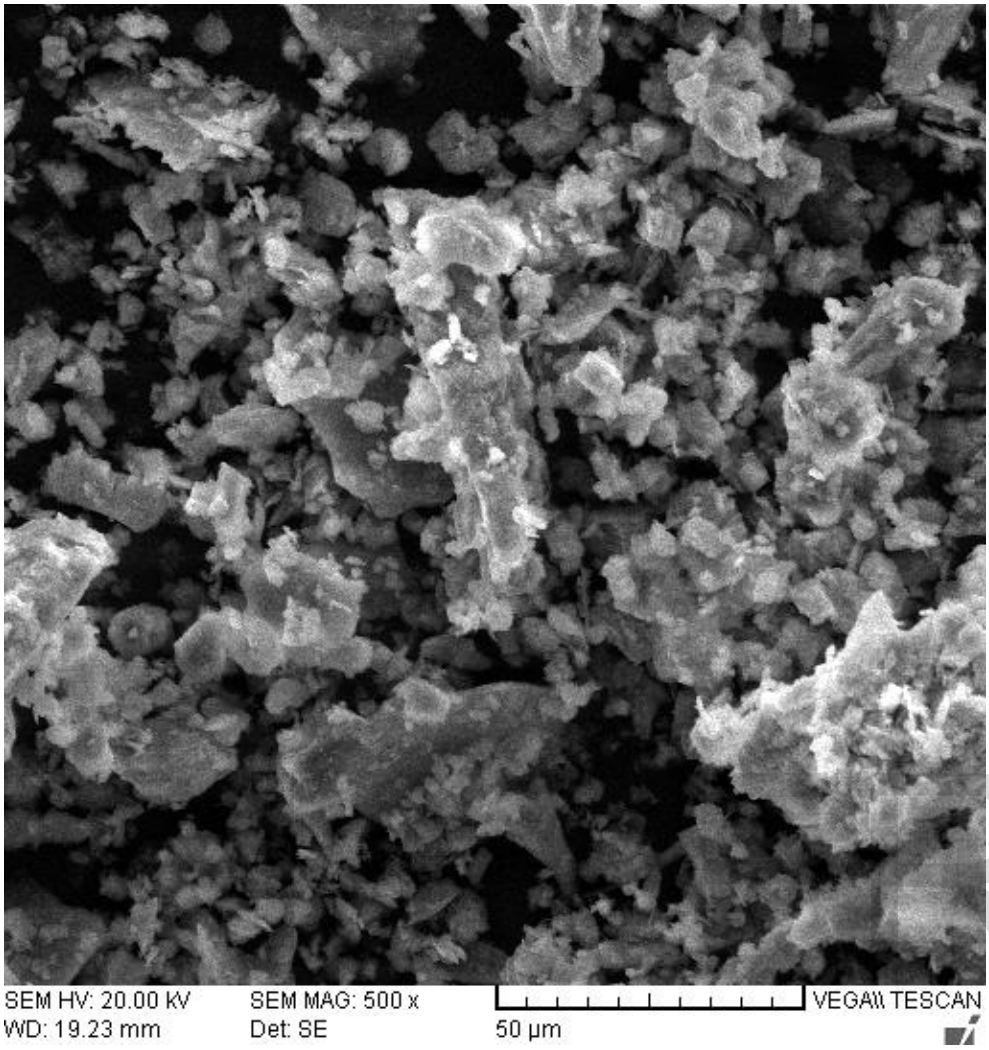

Figure 5: SEM image of the purified Argungu kaolinite

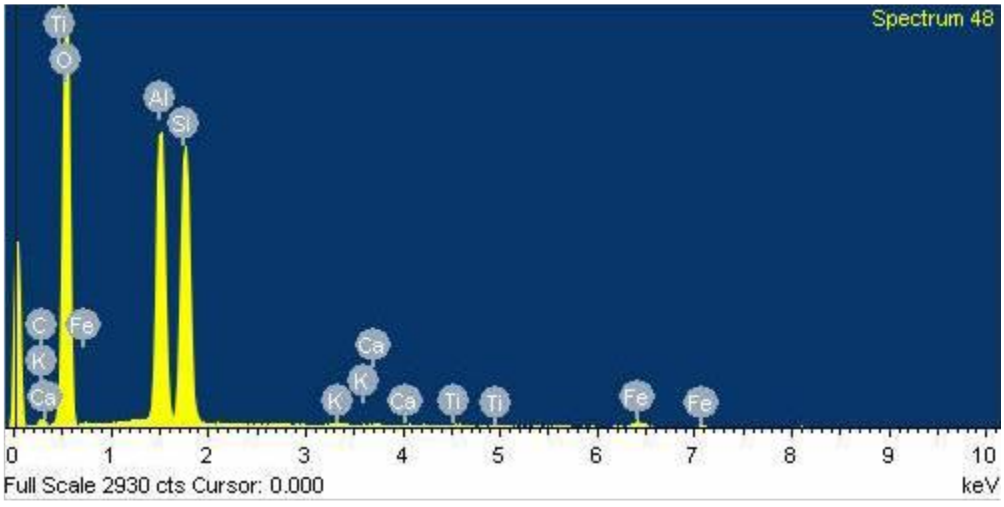

Figure 6: EDS spectrum of the purified Argungu kaolinite

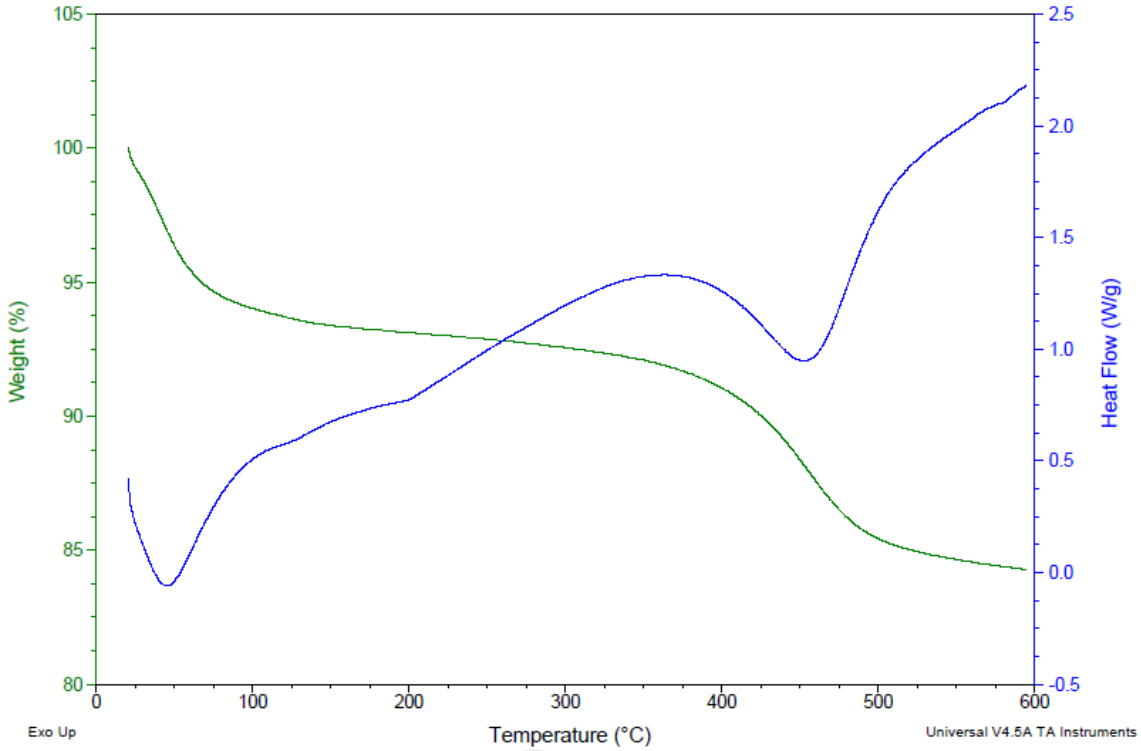

Figure 7: TGA-DSC thermogram of the purified Argungu kaolinite

REFERENCES

1. F. Bergaya, B. Theng and G, Lagaly, *Handbook of clay science*, Amsterdam: Elsevier, pp. 968-1103, **2006**.
2. F. M. Alabi and M. O. Omojola, "Potentials of Nigerian calcined kaolin as paint pigment," *African J. Pure and Appl. Chem.*, 7(12), 410-417, **2013**, doi:10.5897/ajpac2013.0530.
3. F. Naijian, H. Rudi, H. Resalati and H. J. Torshizi, "Application of bio-based modified kaolin clay engineered as paper making additive for improving the properties of filled recycled papers," *Appl. Clay Sci*., 182, 1-10, **2019**, doi:10.1016/j.clay.2019.105258.
4. M. Jiang, X. Jin, X. Lu and Z. Chen, "Adsorption of Pb(II), Cd(II), Ni(II) and Cu(II) onto natural kaolinite clay," *Desalination*, 252, 33-39, **2010**, doi:10.1016/j.desal.2009.11.005.
5. F. A. Dawodu and K. G. Akpomie, "Simultaneous adsorption of Ni(II) and Mn(II) ions from aqueous solution unto a Nigerian kaolinite clay," *J. Mater. Res. Technol.*, 3(2), 129-141, **2014**, doi:10.1016/j.jmrt.2014.03.002.
6. A. Sari and M. Tuzen, "Cd(II) adsorption from aqueous solution by raw and modified kaolinite," *Appl. Clay Sci.*, 88-89, 63-72, **2014**, doi:10.1016/j.clay.2013.12.021.
7. J.Liu, Z. Yun and X. Gui, "Ce/kaolin clay as an active catalyst for fatty acid methyl esters production from cottonseed oil in a new integrated apparatus," *Brazilian J. Chem. Eng.*, 35(1), 147-154, **2018**, http://dx.doi:10.1590/0104-6632.20180351s20160504.
8. A. Sachan and D. Penumadu, "Identification of microfabric of kaolinite clay mineral using X-ray diffraction technique," *Geotech. Geol. Eng.*, 25, 603-616, **2007**, doi:10.1007/s10706-007-9133-8.
9. B. Meroufel, O. Benali, M. Benyahia, Zenasni, M. A. Merlin and B. "George, Removal of Zn (II) from aqueous solution onto kaolin by batch design," *J. Water Res. Protect.*, 5, 669-680, **2013**, doi:10.4236/jwarp.2013.57067.

10. P. Djomgoue and D. Njopwouo, "FT-IR spectroscopy applied for surface clays," *J. Surface Eng. Mater. Adv. Technol.*, 3, 275-282, **2013**, doi:10.4236/jsemat.2013.34037.

11. I. Z. Mukasa-Tebandeke, P. J. M. Ssebuwufu, S. A. Nyanzi, A. Schumann, G. W. A. Nyakairu, M. Ntale and F. Lugolobi, "The Elemental, mineralogical, IR, DTA and XRD analysis characterized clays and clay minerals of Central and Eastern Uganda," *Adv. Mater. Phys. Chem.*, 5, 67-86, **2015**, doi:10.4236/ampc.2015.52010.

12. L. Bouna, A. A. El-Fakir, A. Benlhachemi, K. Draoui, M. Ezahri, B. Bakirz, F Guinneton and N. Elalem, "Synthesis and characterization of mesoporous geopolymer based on Moroccan kaolinite rich clay," *Appl. Clay Sci.*, 196, 1-8, **2020**, doi:10.1016/j.clay.2020.105764.

13. A. K. Panda, B. G. Mishra, D. K. Mishra and R. K. Singh, "Effect of sulphuric acid treatment on the physico-chemical characteristics of kaolin clay," *Coll. Surf. A: Physicochem. Eng. Res. Aspect*., 363, 98-104, **2010**, doi:10.1016/j.colsurfa.2010.04.022.

14. U. Kuila, D. K. McCarty, A. Derkowski, T. B. Fischer, T. Topor and M. Prasad, "Nano-scale texture and porosity of organic matter and clay minerals in organic-rich mudrocks," *Fuel*, 135, 359-373, **2014**, doi:10.1016/j.fuel.2014.06.036

15. F. Macht, K. Eusterhues, G. J. Pronk and K. W. Totsche, "Specific surface area of clay minerals: Comparison between atomic force microscopy measurements and bulk-gas (N_2) and liquid (EGME) adsorption methods," *Appl. Clay Sci.*, 53, 20-26, **2011**, doi:10.1016/j.clay.2011.04.006.

16. U. Kuila and M. Prasad, "Specific surface area and pore-size distribution in clays and shales, *Geophys. Prospecting*, 61, 341-362, **2013**, doi:10.1111/1365-2478.12028.

17. F. O. Nwosu, O. J. Ajala and R. M. Owoyemi, "Preparation and characterization of adsorbents derived from bentonite and kaolin clays," *Appl. Water Sci.*, 8, 195, 1-10, **2018**, doi:10.1007/s13201-018-0827-2.

18. H. R. Akbari, H. Sharafi, A. R. Goodarzi, "Effect of polypropylene fiber inclusion in kaolin clay stabilized with lime and nano-zeolite considering temperatures of 20 and 40 °C," *Bull. Eng. Geol. Environ.*, 80**,** 1841-1855, **2021**, doi:10.1007/s10064-020-02028-x.

19. J. A. Torres-Luna and J. G. Carriazo, "Porous aluminosilicic solids obtained by thermal-acid modification of a commercial kaolinite-type natural clay. *Solid State Sci.*, 88, 29 – 35, **2019**. doi:10.1016/j.solidstatesciences.2018.12.006

20. P. Kamgang-Syapnjeu, D. Njoya, E. Kamseu, L. Cornette-de-Saint, A. Marcano-Zerpa, S. Balme, M. Bechelany and L, Soussan, "Elaboration of a new ceramic membrane support from Cameroonian clays, coconut husks and eggshells: Application for Escherichia coli bacteria retention," *Appl., Clay Sci.*, 198, 105836, **2020**, doi:10.1016/j.clay.2020.105836.

21. H. El-Saied, S. Eel-Sherbiny, O. Ali, W. El-Saied and S. Rohyem, "Preparation of modified kaolin filler with cesium and its application in security Paper," *Adv. Mater. Sci. Eng.*, 2013, 1-7, **2013**, doi:10.1155/2013/274245.

22. N. M. Ahmed, "Comparative study on the role of kaolin, calcined kaolin and chemically treated kaolin in alkyd-based paints for protection of steel," *Pigment & Resin Technol.*, 42(1)1, 3-14, **2013**, doi:10.1108/03699421311288715.

23. J. Dong, Z. Cheng, S. Tan and Q. Zhu, "Clay nanoparticles as pharmaceutical carriers in drug delivery systems," *Expert Opinion on Drug Delivery*, 18(6), 695-714, **2020**, doi:10.1080/17425247.2021.1862792.

24. J. A. Lawal, E. O. Odebunmi and F. A. Adekola, "Adsorption of Fe^{2+}, Pb^{2+}, Zn^{2+} and Cr^{6+} ions from aqueous solutions using natural, ammonium oxalate and sodium hydroxide modified kaolinite clay," *Ife J. Sci.*, 22(3), 1-23, **2020**, doi:10.4314/ijs.v22i3.1.

25. S. A. Hosseini, A. Niaei and D. Salari, "Production of γ-Al_2O_3 from kaolin," *Open J. Phys. Chem.*, 1, 23-27, **2011**, doi:10.4236/ojpc.2011.12004.

26. S. K. Hubadillah, M. H. D. Othman, T. Matsuura, M. A. Rahman, Z. Harun, J. Jaafar and M. Nomura, “Fabrications and applications of low cost ceramic membrane from kaolin: A comprehensive review,” *Ceramics Int.*, 44(5), 4538-4560, **2018**, doi:10.1016/j.ceramint.2017.12.215.